International Journal of Adaptive Control and Signal Processing

WILEY

RESEARCH ARTICLE OPEN ACCESS

An Adaptive Human Pilot Model With Reaction Time Delay for Enhanced Adaptive Control in Piloted Systems

Abdullah Habboush[1,2] | Yildiray Yildiz[1]

[1]Mechanical Engineering Department, Bilkent University, Ankara, Turkey | [2]Mechanical Engineering Department, Eindhoven University of Technology, Eindhoven, the Netherlands

Correspondence: Abdullah Habboush (a.habboush@tue.nl)

Received: 19 February 2025 | **Revised:** 4 December 2025 | **Accepted:** 2 January 2026

Keywords: human pilot modeling | human-in-the-loop | model reference adaptive control | piloted systems | pilot-controller interaction | reaction time delay

ABSTRACT

Adaptive controllers have proven successful in handling uncertain dynamical systems. Yet, their integration into piloted applications remains uncommon owing to their nonlinear characteristics, which give rise to unfavorable interactions between adaptive controllers and human pilots in certain applications. To enable their safe implementation in the loop with human pilots, we introduce an adaptive human pilot model suited for predicting human interactions with adaptive controllers. This model accounts for the time delay in the pilot's response when operating on an adaptive control system, thereby facilitating the evaluation of adaptive controllers in simulation environments and guiding their design to ensure smooth pilot-controller interactions.

1 | Introduction

A human operator's existence in the control loop remains a necessity to date, especially in applications where the inability to cope with uncertainties can lead to tragic outcomes. This is where a prominent branch of control theory known as *model reference adaptive control* (MRAC) proves particularly useful, as it can mitigate the load on human operators. In MRAC, control parameters are updated online in response to deviations from nominal behavior, which can arise due to uncertainties in the plant dynamics. This is achieved by designing update laws that ensure rigorous stability guarantees, and maintain an adequate steady-state performance [1, 2]. However, the special nonlinear characteristics of MRAC can lead to unreliable transients causing unfavorable interactions with human pilots in the loop as reported in previous flight tests [3]. As a result, the implementation of MRAC in piloted applications remains limited, and a need arises for human-in-the-loop analyses that can aid in the design of MRAC for piloted applications.

Human pilot models play a key role in the evaluation of control systems for piloted applications. They enable the testing of controllers in simulation environments and provide guidance throughout the design process. Prominent pilot models like the crossover model [4] and its extensions [5, 6], provide a simple fixed representation of the pilot control decision in the loop with a time-invariant control system. However, when the control system is prone to failure, damage, or sudden parametric changes, these simple pilot models fail to capture how humans are found to adapt in such critical situations. To address these limitations, a few adaptive pilot models have been proposed in the literature.

In [7] and [8], an adaptive pilot model is presented, where the derivation of the update laws is based on expert knowledge such that, in the presence of uncertainty, the adaptive pilot model follows the dictates of the crossover model. This idea was further pursued in [9], where an adaptive pilot model is developed by resorting to the theory of MRAC allowing for a rigorous stability analysis. While the models in [7–9] can capture the adaptive

Abbreviation: MRAC, model reference adaptive control.

behavior of a human pilot in the presence of uncertainty, they are developed by assuming that the pilot operates on a linear control system. Other studies such as [10, 11] and [12] provide a human-in-the-loop stability analysis, where the human operates on an adaptive control system. Yet, the human models in these studies are not adaptive.

One of the earliest adaptive pilot models devised to represent a pilot behavior in the loop with an adaptive control system has been recently proposed in [13]. By employing the theory of MRAC, human update laws are derived based on a rigorous Lyapunov stability analysis. However, this model does not take into consideration the time delay in a pilot's response, which narrows down the class of suitable applications. A pilot's response to visual, aural, or tactile stimuli involves an effective reaction time delay, which includes latencies in the visual, aural, or tactile sensing process, motor nerve conduction time, and central processing time [14]. While the effects of the pilot's reaction time delay can be minimal in certain applications, they are generally significant in a broad class of applications, where the amount of reaction time delay determines the stability of the overall human-in-the-loop dynamics [10, 11].

In this paper, we build upon [13] and propose a novel adaptive pilot model that takes reaction time delay into consideration for a pilot operating on an MRAC control system. The model is suited for the prediction of human interactions with adaptive controllers, which can help in their evaluation and guide in their design. Including the reaction time delay in the adaptive pilot model gives rise to major difficulties, which entail the prediction of the future states of a time-varying uncertain adaptive control system. We resolve this issue through a novel approach, by resorting to the fundamental theory of linear systems, and MRAC, which leads to a rigorous Lyapunov–Krasovskii stability analysis. Furthermore, as pilots deliver their commands through a manipulator, the model also takes into account physical manipulator limits, which impose saturation on the intended pilot commands.

The theoretical results herein were partially presented in a conference version [15]. This paper presents the complete theoretical development of the adaptive pilot model, including the mathematical proofs and elaborate numerical simulations that showcase the efficacy of the presented modeling approach. Furthermore, the proposed adaptive pilot model has also been utilized in [16] to train a deep-learning-based human-autonomy collaboration framework, validated through human-in-the-loop experimental results that demonstrated notable performance improvements.

We start by formulating the problem in Section 2, where the architecture is divided into inner and outer loops. The inner loop is detailed in Section 3, which consists of uncertain plant dynamics and an adaptive controller. Section 4 presents the proposed adaptive human pilot model, which constitutes the outer loop. The main stability result is also provided in this section. Finally, detailed numerical simulations are presented in Section 5, and conclusions are provided in Section 6.

1.1 | Notation

Throughout the paper, $\mathbb{R}^{p\times q}(\mathbb{R}_{+}^{p\times p})[\mathbb{S}^{p\times p}]\{\mathbb{D}^{p\times p}\}$ denotes the set of real (positive-definite real)[symmetric real]{diagonal real} matrices, and $\|.\|$ refers to the euclidean norm for vectors, and the induced-2 norm for matrices. We denote the Frobenius norm for matrices by $\|.\|_F$, the trace operator by $\mathrm{Tr}\{.\}$, and the transpose [inverse] operator by $(.)^T[(.)^{-1}]$. Furthermore, $\lambda_{min}(A)$ refers to the minimum eigenvalue of a matrix A, and $\mathrm{diag}(a) : \mathbb{R}^p \to \mathbb{D}^{p\times p}$ gives a diagonal matrix with $a \in \mathbb{R}^p$ on the diagonal.

Finally, for an update law in the form

$$\dot{\hat{\theta}}(t) = \mathrm{Proj}(\hat{\theta}(t), Y(t)), \tag{1}$$

$\mathrm{Proj}(.,.)$ is the element-wise projection operator, defined in [17], used to bound each element $\hat{\theta}_{i,j}(t)$ of an adaptive parameter $\hat{\theta}(t)$ in a predefined compact set $[\hat{\theta}_{min_{i,j}}, \hat{\theta}_{max_{i,j}}]$.

2 | Problem Formulation

The goal is to model the human control decision when operating on an adaptive control system. Towards that end, we divide the human-in-the-loop architecture into inner and outer loops as shown in Figure 1. The inner loop consists of the plant dynamics of interest, which are controlled by an adaptive control system

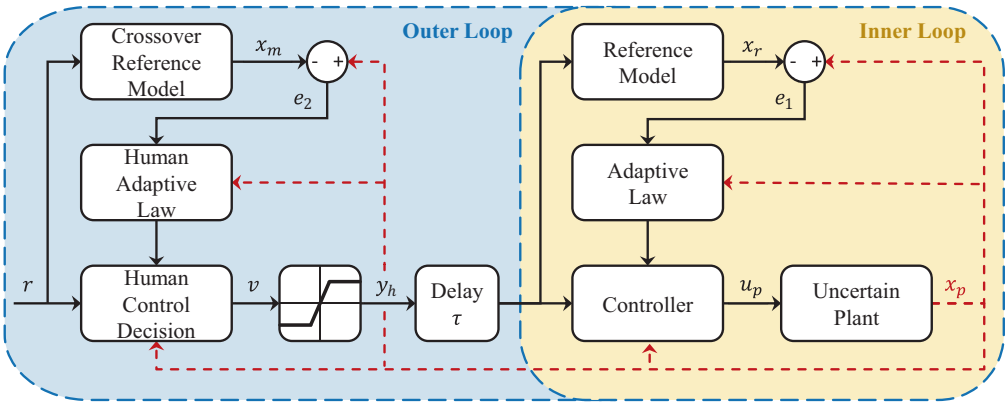

FIGURE 1 | Human-in-the-loop adaptive control system. The outer loop represents human decision-making, while the inner loop includes the plant dynamics and the adaptive controller that tracks the reference model under uncertainty.

to track commands issued by the human in the outer loop. Under the presence of uncertainty in the plant dynamics, deviations arise from the nominal inner-loop behavior, which is prescribed by the reference model. The controller parameters are then updated using the adaptive law such that nominal behavior is restored by tracking the reference model.

The outer loop encloses the human operator that controls the inner loop through a physical manipulator in order to track a desired trajectory and achieve nominal closed-loop dynamics given by the crossover reference model. However, adaptation in the inner loop, due to plant uncertainties, leads to deviations from the crossover reference model, and thus causes the human operator to adapt in an attempt to restore nominal closed-loop behavior. This motivates modeling human adaptation using an MRAC architecture, where human adaptive laws are devised to update the human control decision such that crossover reference model tracking is achieved. Physical manipulator limits impose magnitude saturation on the human control input to the inner loop, and a delay is included to capture the human's reaction time delay. The primary inner- and outer-loop variables used in the human-in-the-loop adaptive control architecture are summarized in Table 1.

TABLE 1 | Summary of primary inner- and outer-loop variables in the human-in-the-loop adaptive control architecture.

Inner-loop variables	
x_p	Accessible plant state vector
u_p	Plant control input
y_1	Plant output of interest for the inner-loop adaptive controller
y_h	Saturated human commands (inner-loop's reference signal)
x_r	State vector of the reference model
e_1	Inner-loop state tracking error
$\hat{K}_x, \hat{\lambda}$	Adaptive parameters of the inner loop controller
γ_x, γ_λ	Inner-loop learning rates
P_1, Q_1	Inner-loop Lyapunov matrices
Outer-loop variables	
y_2	Plant output of interest for human operator
v	Human control decision (unsaturated)
τ	Human reaction time delay
x_m	State vector of the crossover-reference model
e_2	Outer-loop state-tracking error
e_y	Augmented state-tracking error (saturation-compensated)
$\hat{\lambda}_2, \hat{\lambda}_3, \hat{\Phi}_1, \hat{\Phi}_2$	Outer-loop (human) adaptive parameters
$\gamma_2, \gamma_3, \gamma_{\phi_1}, \gamma_{\phi_2}$	Outer-loop (human) learning rates
P_2, Q_2	Outer-loop Lyapunov matrices

3 | Inner Loop

Consider the uncertain plant dynamics

$$\begin{aligned} \dot{x}_p(t) &= A_p x_p(t) + B_p \Lambda u_p(t), \\ y_1(t) &= C_1^T x_p(t), \\ y_2(t) &= C_2^T x_p(t), \end{aligned} \tag{2}$$

where $x_p(t) \in \mathbb{R}^{n_p}$ is the accessible state vector, $u_p(t) \in \mathbb{R}^m$ is the control input, $y_1(t) \in \mathbb{R}^m$ is the output of interest for the adaptive controller, and $y_2(t) \in \mathbb{R}^m$ is the output of interest for the human operator. The state matrix $A_p \in \mathbb{R}^{n_p \times n_p}$ is unknown, and $\Lambda \in \mathbb{R}_+^{m\times m} \cap \mathbb{D}^{m\times m}$ is an unknown control effectiveness matrix with the diagonal elements $\lambda_{i,i} \in (0, 1]$. Furthermore, $B_p \in \mathbb{R}^{n_p \times m}$ is a known control input matrix, $C_1 \in \mathbb{R}^{n_p \times m}$ and $C_2 \in \mathbb{R}^{n_p \times m}$ are known output matrices, and the pair (A_p, B_p) is assumed to be controllable.

The uncertain dynamics (2) reflect the real plant during operation, which is prone to uncertainties. However, nominal dynamics are generally available, which form the starting point for control design. Let the nominal dynamics be known as

$$\dot{x}_r(t) = A_n x_r(t) + B_p u_n(t), \tag{3}$$

where $A_n(t) \in \mathbb{R}^{n_p \times n_p}$ is a known nominal state matrix. Based on (3), a nominal controller $u_n(t) \in \mathbb{R}^m$ is defined as

$$u_n(t) = -L_x x_r(t) + L_r y_h(t - \tau), \tag{4}$$

where the feedback gain $L_x \in \mathbb{R}^{m\times n_p}$ is chosen such that $A_r \triangleq A_n - B_p L_x$ is Hurwitz. The feed-forward gain $L_r \in \mathbb{R}^{m\times m}$ is designed to achieve tracking of human commands $y_h(t - \tau) \in \mathbb{R}^m$, where $\tau \in \mathbb{R}_+$ is the human reaction time delay. The human input $y_h(t)$ is bounded due to physical manipulator limits. It is noted that these bounds are also taken into consideration in the analysis of the outer loop, given in the following section.

The nominal dynamics (3) and (4) constitute the reference model, which can be written as

$$\dot{x}_r(t) = A_r x_r(t) + B_r y_h(t - \tau), \quad x_r(t_0) = 0, \tag{5}$$

where $B_r \triangleq B_p L_r$. The adaptive control objective is to design $u_p(t)$ in (2) to achieve reference model state tracking, that is, $\lim_{t\to\infty} x_p(t) = x_r(t)$. Since (5) is stable, then for a constant human command y_h, the steady state of the reference model satisfies $\lim_{t\to\infty} x_r(t) = -A_r^{-1} B_p L_r y_h$. Hence, achieving $\lim_{t\to\infty} x_p(t) = x_r(t)$ implies that the plant output $y_1(t)$ in (2) takes the form $\lim_{t\to\infty} y_1(t) = -C_1^T A_r^{-1} B_p L_r y_h$. To achieve $\lim_{t\to\infty} y_1(t) = y_h$, we define

$$L_r = -(C_1^T A_r^{-1} B_p)^{-1}. \tag{6}$$

Remark 1. Assigning the feed-forward gain L_r as in (6) to achieve human command following requires the matrix $C_1^T A_r^{-1} B_p$ to be invertible, which is not always possible. We treat such a case in the simulations in Section 5, where a pilot of a 747

airplane feeds pitch-rate commands to the inner loop to achieve a desired pitch-angle trajectory.

To design the adaptive control law $u_p(t)$ for the uncertain dynamics (2), we make the following assumption, which is the standard matching condition.

Assumption 1. There exists a $K_x^* \in \mathbb{R}^{m\times n_p}$ that satisfies the matching condition $A_r = A_p - B_p\Lambda K_x^*$.

Using Assumption 1, and noting that $B_p\Lambda K_r^* = B_r$ for $K_r^* = \Lambda^{-1}L_r$, we define the adaptive control law as

$$u_p(t) = -\hat{K}_x(t)x_p(t) + \mathrm{diag}(\hat{\lambda}(t))L_r y_h(t-\tau), \tag{7}$$

where $\hat{K}_x(t) \in \mathbb{R}^{m\times n_p}$ and $\hat{\lambda}(t) \in \mathbb{R}^m$ are adaptive parameters which serve as estimates for the unknown values K_x^* and λ^*, respectively. Here, $\mathrm{diag}(\lambda^*) = \Lambda^{-1}$, which exists since Λ is a diagonal positive definite matrix.

Substituting (7) into (2) yields

$$\begin{aligned}\dot{x}_p(t) = {} & A_r x_p(t) + B_r y_h(t-\tau) + B_p\Lambda\mathrm{diag}(\tilde{\lambda}(t))L_r y_h(t-\tau)\\ & - B_p\Lambda\tilde{K}_x(t)x_p(t),\end{aligned} \tag{8}$$

where $\tilde{K}_x(t) \triangleq \hat{K}_x(t) - K_x^*$ and $\tilde{\lambda}(t) \triangleq \hat{\lambda}(t) - \lambda^*$. By subtracting (5) from (8), and using $\Lambda\mathrm{diag}(\tilde{\lambda}(t))L_r y_h(t-\tau) = \mathrm{diag}(L_r y_h(t-\tau))\Lambda\tilde{\lambda}(t)$, the error dynamics can be written as

$$\dot{e}_1(t) = A_r e_1(t) + B_p\mathrm{diag}(L_r y_h(t-\tau))\Lambda\tilde{\lambda}(t) - B_p\Lambda\tilde{K}_x(t)x_p(t), \tag{9}$$

where $e_1(t) \triangleq x_p(t) - x_r(t)$ is the inner-loop state-tracking error. Finally, we define the inner-loop adaptive laws as

$$\dot{\hat{K}}_x^T(t) = \dot{\hat{K}}_x^T(t) = \gamma_x x_p(t)e_1(t)^T P_1 B_p, \tag{10a}$$

$$\dot{\hat{\lambda}}(t) = \dot{\hat{\lambda}}(t) = \gamma_\lambda \mathrm{Proj}\Big(\hat{\lambda}(t),\ -\mathrm{diag}(L_r y_h(t-\tau))B_p^T P_1 e_1(t)\Big), \tag{10b}$$

where $\gamma_x, \gamma_\lambda \in \mathbb{R}_+$ are the inner-loop learning rates, and $P_1 \in \mathbb{R}_+^{n_p\times n_p} \cap \mathbb{S}^{n_p\times n_p}$ is the solution of the Lyapunov equation $A_r^T P_1 + P_1 A_r = -Q_1$, for some $Q_1 \in \mathbb{R}_+^{n_p\times n_p} \cap \mathbb{S}^{n_p\times n_p}$. Furthermore, positive bounds $\hat{\lambda}_{max_i}$, $\hat{\lambda}_{min_i} \in \mathbb{R}_+$ are set by the projection operator on each element $\hat{\lambda}_i(t)$, such that $\hat{\lambda}_{max_i} > \hat{\lambda}_i(t) > \hat{\lambda}_{min_i} > 0$ for all $i = 1, \ldots, m$ and $t \geq 0$.

Remark 2. Throughout this paper, without loss of generality, we define all learning rates as scalars instead of diagonal positive definite matrices to maintain simplicity. All results herein apply to the latter, which are also used in the simulations in Section 5.

Lemma 1. *Consider the uncertain dynamical system (2), the reference model (5), and the feedback control law given by (7) and (10). The origin $(e_1 = 0, \tilde{K}_x = 0, \tilde{\lambda} = 0)$ is Lyapunov stable in the large. Furthermore, since the human command $y_h(t)$ is bounded, due to imposed saturation limits by the physical manipulators, $\lim_{t\to\infty} e_1(t) = 0$ and $\dot{\hat{K}}_x(t)$ and $\dot{\hat{\lambda}}(t)$ remain bounded along with all the signals in the inner-loop.*

Proof. The proof of Lemma 1 can be found in [13]. □

4 | Outer Loop

The human operates on the inner-loop dynamics (8), which, by using $\mathrm{diag}(\lambda^*) = \Lambda^{-1}$, can be written as

$$\dot{x}_p(t) = A_r x_p(t) + B_p\Lambda\mathrm{diag}(\hat{\lambda}(t))L_r y_h(t-\tau) - B_p\Lambda\tilde{K}_x(t)x_p(t). \tag{11}$$

We assume that the human operator is well-trained, that is, they are familiar with the nominal inner-loop dynamics given by (5) and the internal time delay τ is known. This implies that, for the human operator, the only unknowns in (11) are Λ, $\hat{\lambda}(t)$ and $\tilde{K}_x(t)$, which constitute the plant uncertainties and the adaptation in the inner loop. Consequently, by defining the unknown time-varying parameters as

$$H^T(t) \triangleq -\Lambda\tilde{K}_x(t), \quad \Lambda_2(t) \triangleq \Lambda\mathrm{diag}(\hat{\lambda}(t)), \tag{12}$$

the inner-loop dynamics (11) can be rewritten as

$$\dot{x}_p(t) = (A_r + B_p H^T(t))x_p(t) + B_p\Lambda_2(t)L_r y_h(t-\tau). \tag{13}$$

Although (13) is a nonlinear adaptive control system, from the human's point of view, it is seen as a linear-time-varying system whose state matrix is $A(t) = A_r + B_p H^T(t)$. The human's objective is to control this system such that the plant states follow the states $x_m(t) \in \mathbb{R}^{n_p}$ of a crossover-reference model given by

$$\dot{x}_m(t) = A_m x_m(t) + B_m r(t-\tau), \tag{14}$$

where $r(t) \in \mathbb{R}^m$ is a bounded reference input representing the desired trajectory the human wants to achieve. Furthermore, $B_m \triangleq B_r\theta_r \in \mathbb{R}^{n_p\times m}$ and $A_m \in \mathbb{R}^{n_p\times n_p}$ is Hurwitz, satisfying the standard matching condition assumption, given below.

Assumption 2. There exists a $\theta_x \in \mathbb{R}^{m\times n_p}$ that satisfies the matching condition $A_m = A_r - B_p L_r\theta_x$.

Similar to the inner loop (see (6)), we define

$$\theta_r = -(C_2^T A_m^{-1} B_r)^{-1}, \tag{15}$$

such that for a constant reference input r, achieving $\lim_{t\to\infty} x_p(t) = x_m(t)$ implies that $\lim_{t\to\infty} y_2(t) = r$. The crossover-reference model captures the nominal closed-loop behavior attained by the human in the absence of uncertainty.

In the ideal case where no saturation is imposed on the human command, and both $H(t)$ and $\Lambda_2(t)$ in (12) are known, the following non-causal human command matches (13) with the crossover-reference model

$$y_h^*(t) = L_r^{-1}\Lambda_2^{-1}(t+\tau)L_r\mathcal{G}^*(t), \tag{16}$$

where

$$\mathcal{G}^*(t) = -\theta_x x_p(t+\tau) + \theta_r r(t) - L_r^{-1}H^T(t+\tau)x_p(t+\tau). \tag{17}$$

While (16) and (17) are not directly applicable due to their dependence on future system variables, they provide a theoretical basis that we use to design the actual human control decision. The

future state of the plant $x_p(t+\tau)$ can be predicted using the solution of the time-varying differential equation (13) as

$$x_p(t+\tau) = \Phi(t+\tau,t)x_p(t) + \int_{-\tau}^{0} \Phi(t+\tau,t+\eta+\tau)B_p\Lambda_2(t+\eta+\tau)L_r y_h(t+\eta)\,\mathrm{d}\eta, \tag{18}$$

where $\Phi(t_2,t_1) \in \mathbb{R}^{n_p\times n_p}$ is the state-transition matrix of (13). Inspired by (16), (17), and (18), we define the saturated human command $y_h(t)$ componentwise as

$$y_{h_i}(t) = \begin{cases} v_i(t), & \text{if } |v_i(t)| \le y_{o_i}, \\ y_{o_i}\mathrm{sgn}(v_i(t)), & \text{if } |v_i(t)| > y_{o_i}, \end{cases} \tag{19}$$

where $y_{h_i}(t)$ is the i^{th} element of the human command vector $y_h(t) = [y_{h_1}(t), \ldots, y_{h_m}(t)]^T$ applied to the inner-loop dynamics (13), and $y_{o_i} \in \mathbb{R}_+$ is the saturation limit of $y_{h_i}(t)$. The unsaturated adaptive human control decision $v(t) = [v_1(t), \ldots, v_m(t)]^T$ is defined as

$$v(t) = L_r^{-1}\mathrm{diag}(\hat{\lambda}_2(t))L_r\mathcal{G}(t), \tag{20}$$

where

$$\mathcal{G}(t) = \hat{\Phi}_1(t)x_p(t) + \theta_r r(t) + \int_{-\tau}^{0} \hat{\Phi}_2(t,\eta)L_r y_h(t+\eta)\,\mathrm{d}\eta. \tag{21}$$

Moreover, $\hat{\Phi}_1(t) \in \mathbb{R}^{m\times n_p}$, $\hat{\Phi}_2(t,\eta) \in \mathbb{R}^{m\times m}$ and $\hat{\lambda}_2(t) \in \mathbb{R}^m$ are adaptive parameters which serve as estimates for the unknown values

$$\begin{aligned} \Phi_1^*(t) &= \overline{H}(t)\Phi(t+\tau,t), \\ \Phi_2^*(t,\eta) &= \overline{H}(t)\Phi(t+\tau,t+\eta+\tau)B_p\Lambda_2(t+\eta+\tau), \end{aligned} \tag{22}$$

and $\lambda_2^*(t)$, respectively, where $\overline{H}(t) \triangleq -(\theta_x + L_r^{-1}H^T(t+\tau))$. Here, $\mathrm{diag}\big(\lambda_2^*(t)\big) = \Lambda_2^{-1}(t+\tau)$, which exists for all $t \ge 0$ since $\Lambda_2(t)$, defined in (12), is diagonal positive definite for all $t \ge 0$. The latter is ensured by using the projection operator in (10b), which bounds the inner-loop adaptive parameter $\hat{\lambda}(t)$ such that it is always positive. The human adaptive control decision (20) is fed through the element-wise saturation function (19) to account for physical manipulator limits.

Substituting (19), (20), and (21) into (13), and after some algebraic manipulations, we get

$$\begin{aligned} \dot{x}_p(t) = {} & A_m x_p(t) + B_m r(t-\tau) + B_p\Lambda_2(t)L_r\Delta y(t-\tau) \\ & + B_p\Lambda_2(t)\mathrm{diag}(\tilde{\lambda}_2(t-\tau))L_r\mathcal{G}(t-\tau) \\ & + B_pL_r\tilde{\Phi}_1(t-\tau)x_p(t-\tau) \\ & + B_pL_r\int_{-\tau}^{0}\tilde{\Phi}_2(t-\tau,\eta)L_r y_h(t+\eta-\tau)\mathrm{d}\eta, \end{aligned} \tag{23}$$

where $\tilde{\Phi}_1(t) \triangleq \hat{\Phi}_1(t) - \Phi_1^*(t)$, $\tilde{\Phi}_2(t,\eta) \triangleq \hat{\Phi}_2(t,\eta) - \Phi_2^*(t,\eta)$ and $\tilde{\lambda}_2(t) \triangleq \hat{\lambda}_2(t) - \lambda_2^*(t)$, and $\Delta y(t) \triangleq y_h(t) - v(t)$ is the control deficiency due to human command saturation. By subtracting (14) from (23), and using $\Lambda_2\mathrm{diag}(\tilde{\lambda}_2)L_r\mathcal{G} = \mathrm{diag}(L_r\mathcal{G})\Lambda_2\tilde{\lambda}_2$, the outer-loop error dynamics can be written as

$$\begin{aligned} \dot{e}_2(t) = {} & A_m e_2(t) + B_p\Lambda_2(t)L_r\Delta y(t-\tau) \\ & + B_p\mathrm{diag}(L_r\mathcal{G}(t-\tau))\Lambda_2(t)\tilde{\lambda}_2(t-\tau) \\ & + B_pL_r\tilde{\Phi}_1(t-\tau)x_p(t-\tau) \\ & + B_pL_r\int_{-\tau}^{0}\tilde{\Phi}_2(t-\tau,\eta)L_r y_h(t+\eta-\tau)\mathrm{d}\eta, \end{aligned} \tag{24}$$

where $e_2(t) \triangleq x_p(t) - x_m(t)$ is the outer-loop state-tracking error.

To remove the effect of control deficiency due to human command saturation from the error dynamics, we generate an auxiliary signal $e_\Delta(t)$ as in [18, 19]

$$\dot{e}_\Delta(t) = A_m e_\Delta(t) + B_p\mathrm{diag}(\hat{\lambda}_3(t))L_r\Delta y(t-\tau), \quad e_\Delta(t_0) = 0, \tag{25}$$

where $\hat{\lambda}_3(t) \in \mathbb{R}^m$ is an adaptive parameter which serves as an estimate for the unknown value $\lambda_3^*(t)$, and $\mathrm{diag}(\lambda_3^*(t)) = \Lambda_2(t)$. Subtracting (25) from (24) and using the fact that $\mathrm{diag}(\tilde{\lambda}_3)L_r\Delta y = \mathrm{diag}(L_r\Delta y)\tilde{\lambda}_3$ yields augmented error dynamics in a standard form

$$\begin{aligned} \dot{e}_y(t) = {} & A_m e_y(t) - B_p\mathrm{diag}(L_r\Delta y(t-\tau))\tilde{\lambda}_3(t) \\ & + B_p\mathrm{diag}(L_r\mathcal{G}(t-\tau))\Lambda_2(t)\tilde{\lambda}_2(t-\tau) \\ & + B_pL_r\tilde{\Phi}_1(t-\tau)x_p(t-\tau) \\ & + B_pL_r\int_{-\tau}^{0}\tilde{\Phi}_2(t-\tau,\eta)L_r y_h(t+\eta-\tau)\mathrm{d}\eta, \end{aligned} \tag{26}$$

where $e_y(t) \triangleq e_2(t) - e_\Delta(t)$ is the augmented error, and $\tilde{\lambda}_3(t) \triangleq \hat{\lambda}_3(t) - \lambda_3^*(t)$. We propose the human adaptive laws

$$\dot{\hat{\lambda}}_2(t) = \gamma_2\mathrm{Proj}\Big(\hat{\lambda}_2(t),\ -\mathrm{diag}(L_r\mathcal{G}(t-\tau))B_p^T P_2 e_y(t)\Big), \tag{27a}$$

$$\dot{\hat{\lambda}}_3(t) = \gamma_3\mathrm{Proj}\Big(\hat{\lambda}_3(t),\ \mathrm{diag}(L_r\Delta y(t-\tau))B_p^T P_2 e_y(t)\Big), \tag{27b}$$

$$\dot{\hat{\Phi}}_1^T(t) = \gamma_{\phi_1}\mathrm{Proj}\Big(\hat{\Phi}_1^T(t),\ -x_p(t-\tau)e_y^T(t)P_2B_pL_r\Big), \tag{27c}$$

$$\dot{\hat{\Phi}}_2^T(t,\eta) = \gamma_{\phi_2}\mathrm{Proj}\Big(\hat{\Phi}_2^T(t,\eta),\ -L_r y_h(t+\eta-\tau)e_y^T(t)P_2B_pL_r\Big), \tag{27d}$$

where $\gamma_2, \gamma_3, \gamma_{\phi_1}, \gamma_{\phi_2} \in \mathbb{R}_+$ are human learning rates, and $P_2 \in \mathbb{R}_+^{n_p\times n_p} \cap \mathbb{S}^{n_p\times n_p}$ is the solution of the Lyapunov equation $A_m^T P_2 + P_2 A_m = -Q_2$, for some $Q_2 \in \mathbb{R}_+^{n_p\times n_p} \cap \mathbb{S}^{n_p\times n_p}$.

The following Lemma and the subsequent remarks play a crucial role in the stability analysis that follows in Theorem 1 below.

Lemma 2. *The state transition matrix $\Phi(t+\tau,t)$ in (18) and its time derivative $\dot{\Phi}(t+\tau,t)$ are bounded, that is, there exist $\phi \in \mathbb{R}_+$ and $\dot{\phi} \in \mathbb{R}_+$ such that $\|\Phi(t+\tau,t)\|_F \le \phi$ and $\|\dot{\Phi}(t+\tau,t)\|_F \le \dot{\phi}$ for all $t \ge t_0$. Additionally, the same bounds apply for $\Phi(t+\tau,t+\eta+\tau)$ and its time derivative, that is, $\|\Phi(t+\tau,t+\eta+\tau)\| \le \phi$ and $\|\dot{\Phi}(t+\tau,t+\eta+\tau)\| \le \dot{\phi}$ for all $t \ge t_0$, $-\tau \le \eta \le 0$.*

Proof. It follows from Lemma 1 that the origin ($e_1 = 0$, $\tilde{K}_x = 0$, $\tilde{\lambda} = 0$) is uniformly stable in the large. The state transition matrix $\Phi(t+\tau,t)$ defines the solution $x_p(t+\tau) = \Phi(t+\tau,t)x_p(t)$ of the homogeneous part of (13)

$$\dot{x}_p(t) = (A_r + B_pH^T(t))x_p(t). \tag{28}$$

Since $x_p(t) = e_1(t) + x_r(t)$, and $x_r(t_0) = 0$, then the homogeneous part of (5)

$$\dot{x}_r(t) = A_r x_r(t), \quad x_r(t_0) = 0, \tag{29}$$

yields the solution $x_r(t) = 0$, which implies that $x_p(t) = e_1(t)$ for all $t \geq t_0$. This shows that the origin $x_p = 0$ of (28) is uniformly stable in the large. It then follows from Theorem 6.4 in [20] that there exists $\phi \in \mathbb{R}_+$ such that $\|\Phi(t_2, t_1)\|_F \leq \phi$ for all $t_1,\ t_2$, where $t_2 \geq t_1$. This in turn implies that

$$\begin{aligned} \|\Phi(t+\tau, t)\|_F &\leq \phi, \qquad \forall\ t \geq t_0, \\ \|\Phi(t+\tau, t+\eta+\tau)\|_F &\leq \phi, \qquad \forall\ t \geq t_0,\ -\tau \leq \eta \leq 0. \end{aligned} \tag{30}$$

Furthermore, the state transition matrix can be defined by the so-called fundamental matrix $X(t)$ of (28) as

$$\Phi(t+\tau, t) = X(t+\tau)X(t)^{-1}, \tag{31}$$

where $X(t)$ is non-singular for all $t \geq t_0$ [21], and satisfies $\dot{X}(t) = A(t)X(t)$. Denoting $A(t) \triangleq (A_r + B_p H^T(t))$, and differentiating (31) yields

$$\begin{aligned} \dot{\Phi}(t+\tau, t) &= \dot{X}(t+\tau)X(t)^{-1} + X(t+\tau)\frac{\mathrm{d}}{\mathrm{d}t}X(t)^{-1} \\ &= \dot{X}(t+\tau)X(t)^{-1} - X(t+\tau)X(t)^{-1}\dot{X}(t)X(t)^{-1} \\ &= A(t+\tau)\Phi(t+\tau, t) - \Phi(t+\tau, t)A(t). \end{aligned} \tag{32}$$

Since the boundedness of $H^T(t) \triangleq -\Lambda \tilde{K}_x(t)$ follows from Lemma 1, then $A(t)$ is also bounded. Together with (30), this shows that all the terms in (32) are bounded, which implies that there exists $\dot{\phi} \in \mathbb{R}_+$ such that

$$\begin{aligned} \|\dot{\Phi}(t+\tau, t)\|_F &\leq \dot{\phi}, \qquad \forall\ t \geq t_0, \\ \|\dot{\Phi}(t+\tau, t+\eta+\tau)\|_F &\leq \dot{\phi}, \qquad \forall\ t \geq t_0,\ -\tau \leq \eta \leq 0. \end{aligned} \tag{33}$$

□

Remark 3. It follows from Lemma 1 that $\tilde{K}(t)$, $\hat{\lambda}(t)$, $\dot{\tilde{K}}(t)$ and $\dot{\hat{\lambda}}(t)$ are bounded, which implies the boundedness of $H(t)$, $\Lambda_2(t)$, $\dot{H}(t)$ and $\dot{\Lambda}_2(t)$. Therefore, there exist $h \in \mathbb{R}_+$, $\dot{h} \in \mathbb{R}_+$, $\beta_3 \in \mathbb{R}_+$ and $\dot{\beta}_3 \in \mathbb{R}_+$ such that $\|H(t)\| \leq h$, $\|\dot{H}(t)\| \leq \dot{h}$, $\|\Lambda_2(t)\|_F \leq \beta_3$ and $\|\dot{\Lambda}_2(t)\|_F \leq \dot{\beta}_3$ for all $t \geq t_0$. The latter implies that $\|\lambda_3^*(t)\| \leq \beta_3$ and $\|\dot{\lambda}_3^*(t)\| \leq \dot{\beta}_3$. Moreover, as $\hat{\lambda}_{min_i} > 0$ for $i = 1, \ldots, m$, there exists $\beta_2 \in \mathbb{R}_+$ such that $\|\Lambda_2^{-1}(t)\|_F \leq \beta_2$. And since $\frac{\mathrm{d}\Lambda_2^{-1}}{\mathrm{d}t} = -\Lambda_2^{-1}\dot{\Lambda}_2\Lambda_2^{-1}$, then there exists $\dot{\beta}_2 \in \mathbb{R}_+$ such that $\|\frac{\mathrm{d}\Lambda_2^{-1}}{\mathrm{d}t}\|_F \leq \dot{\beta}_2$. This implies that $\|\lambda_2^*(t)\| \leq \beta_2$ and $\|\dot{\lambda}_2^*(t)\| \leq \dot{\beta}_2$ for all $t \geq t_0$.

Remark 4. Together with Remark 3, the bounds (30) and (33), established in Lemma 2, show that all the terms of the ideal values (22) and their time derivatives are bounded. Hence, there exist $\phi_1, \dot{\phi}_1, \phi_2, \dot{\phi}_2 \in \mathbb{R}_+$ such that $\|\Phi_1^*(t)\|_F \leq \phi_1$, $\|\dot{\Phi}_1^*(t)\|_F \leq \dot{\phi}_1$ for all $t \geq t_0$, and $\|\Phi_2^*(t, \eta)\|_F \leq \phi_2$, $\|\dot{\Phi}_2^*(t, \eta)\|_F \leq \dot{\phi}_2$ for all $t \geq t_0$, $-\tau \leq \eta \leq 0$.

Theorem 1. *Consider the uncertain dynamical system given by (2), the adaptive controller given by (5), (7) and (10), and the adaptive human pilot model given by (14), (19), (20), (21) and (27). Then, there exists $\tau^* \in \mathbb{R}_+$ such that for all $\tau \in [0,\ \tau^*]$, the solution $(e_y(t), \tilde{\lambda}_2(t), \tilde{\lambda}_3(t), \tilde{\Phi}_1(t), \tilde{\Phi}_2(t, \eta))$ remains bounded for all $t \geq t_0$ and converges to the compact set defined in (59). Furthermore, all closed-loop signals are bounded.*

Proof. Consider the Lyapunov–Krasovskii functional

$$\begin{aligned} V_2 &= e_y^T(t)P_2e_y(t) + \gamma_3^{-1}\tilde{\lambda}_3^T(t)\tilde{\lambda}_3(t) \\ &\quad + \gamma_2^{-1}\tilde{\lambda}_2^T(t)\Lambda_2(t)\tilde{\lambda}_2(t) + \int_{-\tau}^{0}\int_{t+\nu}^{t}\dot{\tilde{\lambda}}_2^T(\xi)\dot{\tilde{\lambda}}_2(\xi)\mathrm{d}\xi\mathrm{d}\nu \\ &\quad + \gamma_{\phi_1}^{-1}\mathrm{Tr}\{\tilde{\Phi}_1^T(t)\tilde{\Phi}_1(t)\} + \int_{-\tau}^{0}\int_{t+\nu}^{t}\mathrm{Tr}\{\dot{\tilde{\Phi}}_1^T(\xi)\dot{\tilde{\Phi}}_1(\xi)\}\mathrm{d}\xi\mathrm{d}\nu \\ &\quad + \gamma_{\phi_2}^{-1}\int_{-\tau}^{0}\mathrm{Tr}\{\tilde{\Phi}_2^T(t, \eta)\tilde{\Phi}_2(t, \eta)\}\mathrm{d}\eta \\ &\quad + \int_{-\tau}^{0}\int_{t+\nu}^{t}\int_{-\tau}^{0}\mathrm{Tr}\{\dot{\tilde{\Phi}}_2^T(\xi, \eta)\dot{\tilde{\Phi}}_2(\xi, \eta)\}\mathrm{d}\eta\mathrm{d}\xi\mathrm{d}\nu. \end{aligned} \tag{34}$$

For brevity, we define

$$\begin{aligned} W(t) &\triangleq \int_{-\tau}^{0}\int_{t+\nu}^{t}\dot{\tilde{\lambda}}_2^T(\xi)\dot{\tilde{\lambda}}_2(\xi)\mathrm{d}\xi\mathrm{d}\nu + \int_{-\tau}^{0}\int_{t+\nu}^{t}\mathrm{Tr}\{\dot{\tilde{\Phi}}_1^T(\xi)\dot{\tilde{\Phi}}_1(\xi)\}\mathrm{d}\xi\mathrm{d}\nu \\ &\quad + \int_{-\tau}^{0}\int_{t+\nu}^{t}\int_{-\tau}^{0}\mathrm{Tr}\{\dot{\tilde{\Phi}}_2^T(\xi, \eta)\dot{\tilde{\Phi}}_2(\xi, \eta)\}\mathrm{d}\eta\mathrm{d}\xi\mathrm{d}\nu, \end{aligned} \tag{35}$$

where

$$\begin{aligned} \dot{W}(t) &= \tau\dot{\tilde{\lambda}}_2^T(t)\dot{\tilde{\lambda}}_2(t) - \int_{-\tau}^{0}\dot{\tilde{\lambda}}_2^T(t+\nu)\dot{\tilde{\lambda}}_2(t+\nu)\mathrm{d}\nu \\ &\quad + \tau\mathrm{Tr}\left\{\dot{\tilde{\Phi}}_1^T(t)\dot{\tilde{\Phi}}_1(t)\right\} - \int_{-\tau}^{0}\mathrm{Tr}\{\dot{\tilde{\Phi}}_1^T(t+\nu)\dot{\tilde{\Phi}}_1(t+\nu)\}\mathrm{d}\nu \\ &\quad + \tau\int_{-\tau}^{0}\mathrm{Tr}\{\dot{\tilde{\Phi}}_2^T(t, \eta)\dot{\tilde{\Phi}}_2(t, \eta)\}\mathrm{d}\eta \\ &\quad - \int_{-\tau}^{0}\int_{-\tau}^{0}\mathrm{Tr}\{\dot{\tilde{\Phi}}_2^T(t+\nu, \eta)\dot{\tilde{\Phi}}_2(t+\nu, \eta)\}\mathrm{d}\eta\mathrm{d}\nu. \end{aligned} \tag{36}$$

Differentiating (34) along the trajectories (26) and (27), and using (36), we obtain that

$$\begin{aligned} \dot{V}_2 &= -e_y^T(t)Q_2e_y(t) - 2\tilde{\lambda}_3^T(t)\mathrm{diag}(L_r\Delta y(t-\tau))B_p^TP_2e_y(t) \\ &\quad + 2\tilde{\lambda}_2^T(t-\tau)\Lambda_2(t)\mathrm{diag}(L_r\mathcal{G}(t-\tau))B_p^TP_2e_y(t) \\ &\quad + 2e_y^T(t)P_2B_pL_r\tilde{\Phi}_1(t-\tau)x_p(t-\tau) \\ &\quad + 2e_y^T(t)P_2B_pL_r\int_{-\tau}^{0}\tilde{\Phi}_2(t-\tau, \eta)L_ry_h(t+\eta-\tau)\mathrm{d}\eta \\ &\quad + 2\gamma_3^{-1}\tilde{\lambda}_3^T(t)\dot{\tilde{\lambda}}_3(t) \\ &\quad + 2\gamma_{\phi_1}^{-1}\mathrm{Tr}\{\dot{\tilde{\Phi}}_1^T(t)\tilde{\Phi}_1(t)\} \\ &\quad + 2\gamma_2^{-1}\tilde{\lambda}_2^T(t)\Lambda_2(t)\dot{\tilde{\lambda}}_2(t) \\ &\quad + \gamma_2^{-1}\tilde{\lambda}_2^T(t)\dot{\Lambda}_2(t)\tilde{\lambda}_2(t) \\ &\quad + 2\gamma_{\phi_2}^{-1}\int_{-\tau}^{0}\mathrm{Tr}\{\dot{\tilde{\Phi}}_2^T(t, \eta)\tilde{\Phi}_2(t, \eta)\}\mathrm{d}\eta + \dot{W}(t). \end{aligned} \tag{37}$$

Using the fact that $g(t-\tau) = g(t) - \int_{-\tau}^{0}\dot{g}(t+\nu)\mathrm{d}\nu$ for $\tilde{\lambda}_2^T(t-\tau)$, $\tilde{\Phi}_1(t-\tau)$ and $\tilde{\Phi}_2(t-\tau, \eta)$, and decomposing $\dot{\tilde{\lambda}}_2(t) = \dot{\hat{\lambda}}_2(t) - \dot{\lambda}_2^*(t)$, $\dot{\tilde{\lambda}}_3(t) = \dot{\hat{\lambda}}_3(t) - \dot{\lambda}_3^*(t)$, $\dot{\tilde{\Phi}}_1(t) = \dot{\hat{\Phi}}_1(t) - \dot{\Phi}_1^*(t)$ and $\dot{\tilde{\Phi}}_2(t, \eta) = \dot{\hat{\Phi}}_2(t, \eta) - \dot{\Phi}_2^*(t, \eta)$, we get

$$\begin{aligned} \dot{V}_2 &= -e_y^T(t)Q_2e_y(t) - 2\tilde{\lambda}_3^T(t)\mathrm{diag}(L_r\Delta y(t-\tau))B_p^TP_2e_y(t) \\ &\quad + 2\tilde{\lambda}_2^T(t)\Lambda_2(t)\mathrm{diag}(L_r\mathcal{G}(t-\tau))B_p^TP_2e_y(t) \\ &\quad - 2\left(\int_{-\tau}^{0}\dot{\tilde{\lambda}}_2^T(t+\nu)\mathrm{d}\nu\right)\Lambda_2(t)\mathrm{diag}(L_r\mathcal{G}(t-\tau))B_p^TP_2e_y(t) \\ &\quad + 2e_y^T(t)P_2B_pL_r\left[\tilde{\Phi}_1(t)x_p(t-\tau) - \left(\int_{-\tau}^{0}\dot{\tilde{\Phi}}_1(t+\nu)\mathrm{d}\nu\right)\right. \end{aligned}$$

$$
\begin{aligned}
&x_p(t-\tau)+\int_{-\tau}^{0}\tilde{\Phi}_2(t,\eta)L_r y_h(t+\eta-\tau)\mathrm{d}\eta\\
&-\int_{-\tau}^{0}\left(\int_{-\tau}^{0}\dot{\tilde{\Phi}}_2(t+\nu,\eta)\mathrm{d}\nu\right)L_r y_h(t+\eta-\tau)\mathrm{d}\eta\Big]\\
&+2\gamma_3^{-1}\tilde{\lambda}_3^T(t)\dot{\hat{\lambda}}_3(t)-2\gamma_3^{-1}\tilde{\lambda}_3^T(t)\dot{\lambda}_3^*(t)+2\gamma_2^{-1}\tilde{\lambda}_2^T(t)\Lambda_2(t)\dot{\hat{\lambda}}_2(t)\\
&-2\gamma_2^{-1}\tilde{\lambda}_2^T(t)\Lambda_2(t)\dot{\lambda}_2^*(t)\\
&+\gamma_2^{-1}\tilde{\lambda}_2^T(t)\dot{\Lambda}_2(t)\tilde{\lambda}_2(t)+2\gamma_{\phi_1}^{-1}\mathrm{Tr}\{\dot{\tilde{\Phi}}_1^T(t)\tilde{\Phi}_1(t)\}\\
&-2\gamma_{\phi_1}^{-1}\mathrm{Tr}\left\{\dot{\Phi}_1^{*T}(t)\tilde{\Phi}_1(t)\right\}\\
&+2\gamma_{\phi_2}^{-1}\int_{-\tau}^{0}\mathrm{Tr}\{\dot{\tilde{\Phi}}_2^T(t,\eta)\tilde{\Phi}_2(t,\eta)\}\mathrm{d}\eta-2\gamma_{\phi_2}^{-1}\\
&\int_{-\tau}^{0}\mathrm{Tr}\{\dot{\Phi}_2^{*T}(t,\eta)\tilde{\Phi}_2(t,\eta)\}\mathrm{d}\eta+\dot{W}(t).
\end{aligned}
\tag{38}
$$

Defining

$$
\begin{aligned}
N^*(t)\triangleq&\gamma_2^{-1}\tilde{\lambda}_2^T(t)\dot{\Lambda}_2(t)\tilde{\lambda}_2(t)-2\gamma_2^{-1}\tilde{\lambda}_2^T(t)\Lambda_2(t)\dot{\lambda}_2^*(t)\\
&-2\gamma_3^{-1}\tilde{\lambda}_3^T(t)\dot{\lambda}_3^*(t)-2\gamma_{\phi_1}^{-1}\mathrm{Tr}\left\{\dot{\Phi}_1^{*T}(t)\tilde{\Phi}_1(t)\right\}\\
&-2\gamma_{\phi_2}^{-1}\int_{-\tau}^{0}\mathrm{Tr}\{\dot{\Phi}_2^{*T}(t,\eta)\tilde{\Phi}_2(t,\eta)\}\mathrm{d}\eta,
\end{aligned}
\tag{39}
$$

using $\mathrm{Tr}(AB)=\mathrm{Tr}(BA)$ and rearranging, we get

$$
\begin{aligned}
\dot{V}_2=&-e_y^T(t)Q_2e_y(t)+N^*(t)+\dot{W}(t)\\
&+2\tilde{\lambda}_3^T(t)\Big(-\mathrm{diag}(L_r\Delta y(t-\tau))B_p^TP_2e_y(t)+\gamma_3^{-1}\dot{\hat{\lambda}}_3(t)\Big)\\
&+2\tilde{\lambda}_2^T(t)\Lambda_2(t)\Big(\mathrm{diag}(L_r\mathcal{G}(t-\tau))B_p^TP_2e_y(t)+\gamma_2^{-1}\dot{\hat{\lambda}}_2(t)\Big)\\
&+2\mathrm{Tr}\left\{\tilde{\Phi}_1(t)\Big(x_p(t-\tau)e_y^T(t)P_2B_pL_r+\gamma_{\phi_1}^{-1}\dot{\tilde{\Phi}}_1^T(t)\Big)\right\}\\
&+2\int_{-\tau}^{0}\mathrm{Tr}\Big\{\tilde{\Phi}_2(t,\eta)\Big(L_ry_h(t+\eta-\tau)e_y^T(t)P_2B_pL_r\\
&+\gamma_{\phi_2}^{-1}\dot{\tilde{\Phi}}_2^T(t,\eta)\Big)\Big\}\mathrm{d}\eta\\
&-2\int_{-\tau}^{0}\dot{\tilde{\lambda}}_2^T(t+\nu)\Lambda_2(t)\mathrm{diag}(L_r\mathcal{G}(t-\tau))B_p^TP_2e_y(t)\mathrm{d}\nu\\
&-2\int_{-\tau}^{0}\mathrm{Tr}\{\dot{\tilde{\Phi}}_1(t+\nu)x_p(t-\tau)e_y^T(t)P_2B_pL_r\}\mathrm{d}\nu\\
&-2\int_{-\tau}^{0}\int_{-\tau}^{0}\mathrm{Tr}\{\dot{\tilde{\Phi}}_2(t+\nu,\eta)L_ry_h(t+\eta-\tau)\\
&e_y^T(t)P_2B_pL_r\}\mathrm{d}\nu\mathrm{d}\eta.
\end{aligned}
\tag{40}
$$

Substituting the adaptive laws (27) in (40) yields

$$
\begin{aligned}
\dot{V}_2=&-e_y^T(t)Q_2e_y(t)+N^*(t)+\dot{W}(t)\\
&+2\tilde{\lambda}_3^T(t)\big(\mathrm{Proj}(\hat{\lambda}_3(t),\ Y_3(t))-Y_3(t)\big)\\
&+2\tilde{\lambda}_2^T(t)\Lambda_2(t)\big(\mathrm{Proj}(\hat{\lambda}_2(t),\ Y_2(t))-Y_2(t)\big)\\
&+2\mathrm{Tr}\left\{\tilde{\Phi}_1(t)\big(\mathrm{Proj}(\hat{\Phi}_1(t),\ Y_{\phi_1}(t))-Y_{\phi_1}(t)\big)\right\}\\
&+2\int_{-\tau}^{0}\mathrm{Tr}\{\tilde{\Phi}_2(t,\eta)\big(\mathrm{Proj}(\hat{\Phi}_2(t,\eta),\ Y_{\phi_2}(t,\eta))\\
&-Y_{\phi_2}(t,\eta)\big)\}\mathrm{d}\eta\\
&+2\int_{-\tau}^{0}\dot{\tilde{\lambda}}_2^T(t+\nu)\Lambda_2(t)Y_2(t)\mathrm{d}\nu\\
&+2\int_{-\tau}^{0}\mathrm{Tr}\{\dot{\tilde{\Phi}}_1(t+\nu)Y_{\phi_1}(t)\}\mathrm{d}\nu\\
&+2\int_{-\tau}^{0}\int_{-\tau}^{0}\mathrm{Tr}\{\dot{\tilde{\Phi}}_2(t+\nu,\eta)Y_{\phi_2}(t,\eta)\}\mathrm{d}\nu\mathrm{d}\eta,
\end{aligned}
\tag{41}
$$

where

$$
\begin{aligned}
Y_2(t)&\triangleq-\mathrm{diag}(L_r\mathcal{G}(t-\tau))B_p^TP_2e_y(t),\\
Y_3(t)&\triangleq\mathrm{diag}(L_r\Delta y(t-\tau))B_p^TP_2e_y(t),\\
Y_{\phi_1}(t)&\triangleq-x_p(t-\tau)e_y^T(t)P_2B_pL_r,\\
Y_{\phi_2}(t,\eta)&\triangleq-L_ry_h(t+\eta-\tau)e_y^T(t)P_2B_pL_r.
\end{aligned}
\tag{42}
$$

Using the projection property $(\theta_{i,j}-\theta_{i,j}^*)(\mathrm{Proj}(\theta_{i,j},Y_{i,j})-Y_{i,j})\le 0$ [17], and the fact that $\Lambda_2(t)$ is diagonal positive definite, it follows from (41) that

$$
\begin{aligned}
\dot{V}_2\le&-e_y^T(t)Q_2e_y(t)+N^*(t)+\dot{W}(t)\\
&+2\int_{-\tau}^{0}\dot{\tilde{\lambda}}_2^T(t+\nu)\Lambda_2(t)Y_2(t)\mathrm{d}\nu\\
&+2\int_{-\tau}^{0}\mathrm{Tr}\{\dot{\tilde{\Phi}}_1(t+\nu)Y_{\phi_1}(t)\}\mathrm{d}\nu\\
&+2\int_{-\tau}^{0}\int_{-\tau}^{0}\mathrm{Tr}\{\dot{\tilde{\Phi}}_2(t+\nu,\eta)Y_{\phi_2}(t,\eta)\}\mathrm{d}\nu\mathrm{d}\eta.
\end{aligned}
$$

Using the algebraic inequality $\mathrm{Tr}\{2A^TB\}\le\mathrm{Tr}\{A^TA+B^TB\}$, we obtain that

$$
\begin{aligned}
\dot{V}_2\le&-e_y^T(t)Q_2e_y(t)+N^*(t)+\dot{W}(t)\\
&+\int_{-\tau}^{0}\dot{\tilde{\lambda}}_2^T(t+\nu)\dot{\tilde{\lambda}}_2(t+\nu)\mathrm{d}\nu\\
&+\int_{-\tau}^{0}Y_2^T(t)\Lambda_2(t)\Lambda_2(t)Y_2(t)\mathrm{d}\nu\\
&+\int_{-\tau}^{0}\mathrm{Tr}\{\dot{\tilde{\Phi}}_1^T(t+\nu)\dot{\tilde{\Phi}}_1(t+\nu)\}\mathrm{d}\nu\\
&+\int_{-\tau}^{0}\mathrm{Tr}\{Y_{\phi_1}^T(t)Y_{\phi_1}(t)\}\mathrm{d}\nu\\
&+\int_{-\tau}^{0}\int_{-\tau}^{0}\mathrm{Tr}\{\dot{\tilde{\Phi}}_2^T(t+\nu,\eta)\dot{\tilde{\Phi}}_2(t+\nu,\eta)\}\mathrm{d}\nu\mathrm{d}\eta\\
&+\int_{-\tau}^{0}\int_{-\tau}^{0}\mathrm{Tr}\{Y_{\phi_2}^T(t,\eta)Y_{\phi_2}(t,\eta)\}\mathrm{d}\nu\mathrm{d}\eta.
\end{aligned}
\tag{43}
$$

Substituting (36) in (43) yields

$$
\begin{aligned}
\dot{V}_2\le&-e_y^T(t)Q_2e_y(t)+N^*(t)\\
&+\tau Y_2^T(t)\Lambda_2(t)\Lambda_2(t)Y_2(t)\\
&+\tau\mathrm{Tr}\{Y_{\phi_1}^T(t)Y_{\phi_1}(t)\}\\
&+\tau\int_{-\tau}^{0}\mathrm{Tr}\{Y_{\phi_2}^T(t,\eta)Y_{\phi_2}(t,\eta)\}\mathrm{d}\eta\\
&+\tau\dot{\tilde{\lambda}}_2^T(t)\dot{\tilde{\lambda}}_2(t)\\
&+\tau\mathrm{Tr}\left\{\dot{\tilde{\Phi}}_1^T(t)\dot{\tilde{\Phi}}_1(t)\right\}\\
&+\tau\int_{-\tau}^{0}\mathrm{Tr}\{\dot{\tilde{\Phi}}_2^T(t,\eta)\dot{\tilde{\Phi}}_2(t,\eta)\}\mathrm{d}\eta.
\end{aligned}
\tag{44}
$$

Using the algebraic inequality

$$\begin{aligned}\mathrm{Tr}\left\{\dot{\hat{\Phi}}_1^T(t)\dot{\hat{\Phi}}_1(t)\right\} &= \mathrm{Tr}\left\{\dot{\hat{\Phi}}_1^T(t)\dot{\hat{\Phi}}_1(t)\right\} + \mathrm{Tr}\left\{\dot{\Phi}_1^{*T}(t)\dot{\Phi}_1^*(t)\right\} \\ &\quad - 2\mathrm{Tr}\left\{\dot{\hat{\Phi}}^T(t)\dot{\Phi}^*(t)\right\} \\ &\le 2\mathrm{Tr}\{\dot{\hat{\Phi}}_1^T(t)\dot{\hat{\Phi}}_1(t)\} + 2\mathrm{Tr}\left\{\dot{\Phi}_1^{*T}(t)\dot{\Phi}_1^*(t)\right\},\end{aligned}$$

for the last three terms in (44), one can write

$$\begin{aligned}\dot{V}_2 \le & -e_y^T(t)Q_2e_y(t) + N^*(t) + \tau Y_2^T(t)\Lambda_2(t)\Lambda_2(t)Y_2(t) \\ & + \tau\mathrm{Tr}\{Y_{\phi_1}^T(t)Y_{\phi_1}(t)\} + \tau\int_{-\tau}^{0}\mathrm{Tr}\{Y_{\phi_2}^T(t,\eta)Y_{\phi_2}(t,\eta)\}\mathrm{d}\eta \\ & + 2\tau\dot{\hat{\lambda}}_2^T(t)\dot{\hat{\lambda}}_2(t) + 2\tau\dot{\lambda}_2^{*T}(t)\dot{\lambda}_2^*(t) \\ & + 2\tau\mathrm{Tr}\{\dot{\hat{\Phi}}_1^T(t)\dot{\hat{\Phi}}_1(t)\} + 2\tau\mathrm{Tr}\left\{\dot{\Phi}_1^{*T}(t)\dot{\Phi}_1^*(t)\right\} \\ & + 2\tau\int_{-\tau}^{0}\mathrm{Tr}\left\{\dot{\hat{\Phi}}_2^T(t,\eta)\dot{\hat{\Phi}}_2(t,\eta)\right\}\mathrm{d}\eta \\ & + 2\tau\int_{-\tau}^{0}\mathrm{Tr}\left\{\dot{\Phi}_2^{*T}(t,\eta)\dot{\Phi}_2^*(t,\eta)\right\}\mathrm{d}\eta. \end{aligned} \tag{45}$$

Let $Y_2(t) = [a_1(t), \ldots, a_m(t)]^T$ and $\Lambda_2(t) = \mathrm{diag}([b_1(t), \ldots, b_m(t)])$ for some $a_i(t) \in \mathbb{R}$, $b_i(t) \in \mathbb{R}_+$, for $i = 1, \ldots, m$. Since $\Lambda_2(t)$, defined in (12), is shown to be bounded in Remark 3, then $b_i(t) \le \lambda_{i,i}\hat{\lambda}_{max_i}$ for all $t \ge t_0$, $i = 1, \ldots, m$, where $\lambda_{i,i}$ is the i^{th} diagonal element of Λ, and $\hat{\lambda}_{max_i}$ is the i^{th} projection upper bound of $\hat{\lambda}(t)$ in (10b). Then, one can write

$$\begin{aligned}Y_2^T(t)\Lambda_2(t)\Lambda_2(t)Y_2(t) &= b_1^2(t)a_1^2(t) + \cdots + b_m^2(t)a_m^2(t) \\ &\le \mu(a_1^2(t) + \cdots + a_m^2(t)) = \mu Y_2^T(t)Y_2(t),\end{aligned} \tag{46}$$

where $\mu \triangleq \max_i(\lambda_{i,i}\hat{\lambda}_{max_i})^2$. Furthermore, using the property that the projection operator bounds an adaptive parameter in a compact set, then from the element-wise projection operator's definition in [17], it can be shown that

$$\mathrm{Tr}\{\dot{\hat{\Phi}}_1^T(t)\dot{\hat{\Phi}}_1(t)\} \le \gamma_{\phi_1}^2\,\mathrm{Tr}\{Y_{\phi_1}^T(t)Y_{\phi_1}(t)\}. \tag{47}$$

Using (46) and (47) in (45), we obtain that

$$\begin{aligned}\dot{V}_2 \le & -e_y^T(t)Q_2e_y(t) + N^*(t) \\ & + \tau(\mu + 2\gamma_2^2)Y_2^T(t)Y_2(t) + \tau(1+2\gamma_{\phi_1}^2)\mathrm{Tr}\{Y_{\phi_1}^T(t)Y_{\phi_1}(t)\} \\ & + \tau(1+2\gamma_{\phi_2}^2)\int_{-\tau}^{0}\mathrm{Tr}\{Y_{\phi_2}^T(t,\eta)Y_{\phi_2}(t,\eta)\}\mathrm{d}\eta \\ & + 2\tau\dot{\lambda}_2^{*T}(t)\dot{\lambda}_2^*(t) + 2\tau\mathrm{Tr}\left\{\dot{\Phi}_1^{*T}(t)\dot{\Phi}_1^*(t)\right\} \\ & + 2\tau\int_{-\tau}^{0}\mathrm{Tr}\left\{\dot{\Phi}_2^{*T}(t,\eta)\dot{\Phi}_2^*(t,\eta)\right\}\mathrm{d}\eta. \end{aligned} \tag{48}$$

Using the property $\mathrm{Tr}\{Y^TY\} = \|Y\|_F^2$ for a matrix Y, we can rewrite (48) as

$$\begin{aligned}\dot{V}_2 \le & -e_y^T(t)Q_2e_y(t) + N^*(t) \\ & + \tau(\mu + 2\gamma_2^2)\|Y_2(t)\|^2 + \tau(1+2\gamma_{\phi_1}^2)\|Y_{\phi_1}(t)\|_F^2 \\ & + \tau(1+2\gamma_{\phi_2}^2)\int_{-\tau}^{0}\|Y_{\phi_2}(t,\eta)\|_F^2\mathrm{d}\eta \\ & + 2\tau\dot{\lambda}_2^{*T}(t)\dot{\lambda}_2^*(t) + 2\tau\mathrm{Tr}\left\{\dot{\Phi}_1^{*T}(t)\dot{\Phi}_1^*(t)\right\} \\ & + 2\tau\int_{-\tau}^{0}\mathrm{Tr}\left\{\dot{\Phi}_2^{*T}(t,\eta)\dot{\Phi}_2^*(t,\eta)\right\}\mathrm{d}\eta. \end{aligned} \tag{49}$$

Substituting (42) into (49), yields

$$\begin{aligned}\dot{V}_2 \le & -\lambda_{min}(Q_2)\|e_y(t)\|^2 + N^*(t) \\ & + \tau(\mu + 2\gamma_2^2)\|\mathrm{diag}(L_r\mathcal{G}(t-\tau))\|^2\|P_2B_p\|^2\|e_y(t)\|^2 \\ & + \tau(1+2\gamma_{\phi_1}^2)\|x_p(t-\tau)\|^2\|e_y(t)\|^2\|P_2B_pL_r\|_F^2 \\ & + \tau(1+2\gamma_{\phi_2}^2)\int_{-\tau}^{0}\|L_ry_h(t+\eta-\tau)\|^2\|e_y(t)\|^2\|P_2B_pL_r\|_F^2\mathrm{d}\eta \\ & + 2\tau\dot{\lambda}_2^{*T}(t)\dot{\lambda}_2^*(t) + 2\tau\mathrm{Tr}\left\{\dot{\Phi}_1^{*T}(t)\dot{\Phi}_1^*(t)\right\} \\ & + 2\tau\int_{-\tau}^{0}\mathrm{Tr}\left\{\dot{\Phi}_2^{*T}(t,\eta)\dot{\Phi}_2^*(t,\eta)\right\}\mathrm{d}\eta. \end{aligned} \tag{50}$$

Substituting (39) for $N^*(t)$ in (50), yields

$$\begin{aligned}\dot{V}_2 \le & -\lambda_{min}(Q_2)\|e_y(t)\|^2 + \tau(\mu + 2\gamma_2^2) \\ & \|\mathrm{diag}(L_r\mathcal{G}(t-\tau))\|^2\|P_2B_p\|^2\|e_y(t)\|^2 \\ & + \tau(1+2\gamma_{\phi_1}^2)\|x_p(t-\tau)\|^2\|e_y(t)\|^2\|P_2B_pL_r\|_F^2 \\ & + \tau(1+2\gamma_{\phi_2}^2)\int_{-\tau}^{0}\|L_ry_h(t+\eta-\tau)\|^2 \\ & \|e_y(t)\|^2\|P_2B_pL_r\|_F^2\mathrm{d}\eta \\ & + 2\tau\dot{\lambda}_2^{*T}(t)\dot{\lambda}_2^*(t) + 2\tau\mathrm{Tr}\left\{\dot{\Phi}_1^{*T}(t)\dot{\Phi}_1^*(t)\right\} \\ & + 2\tau\int_{-\tau}^{0}\mathrm{Tr}\left\{\dot{\Phi}_2^{*T}(t,\eta)\dot{\Phi}_2^*(t,\eta)\right\}\mathrm{d}\eta \\ & + \gamma_2^{-1}\dot{\tilde{\lambda}}_2^T(t)\dot{\Lambda}_2(t)\tilde{\lambda}_2(t) - 2\gamma_2^{-1}\tilde{\lambda}_2^T(t)\Lambda_2(t)\dot{\lambda}_2^*(t) \\ & - 2\gamma_3^{-1}\tilde{\lambda}_3^T(t)\dot{\lambda}_3^*(t) - 2\gamma_{\phi_1}^{-1}\mathrm{Tr}\left\{\dot{\Phi}_1^{*T}(t)\tilde{\Phi}_1(t)\right\} \\ & - 2\gamma_{\phi_2}^{-1}\int_{-\tau}^{0}\mathrm{Tr}\{\dot{\Phi}_2^{*T}(t,\eta)\tilde{\Phi}_2(t,\eta)\}\mathrm{d}\eta. \end{aligned} \tag{51}$$

Using Remarks 3 and 4, and denoting $p \triangleq \max(\|P_2B_p\|^2, \|P_2B_pL_r\|_F^2)$, yields

$$\begin{aligned}\dot{V}_2 \le & -\lambda_{min}(Q_2)\|e_y(t)\|^2 + \tau p(\mu + 2\gamma_2^2) \\ & \|\mathrm{diag}(L_r\mathcal{G}(t-\tau))\|^2\|e_y(t)\|^2 \\ & + \tau p(1+2\gamma_{\phi_1}^2)\|x_p(t-\tau)\|^2\|e_y(t)\|^2 \\ & + \tau p(1+2\gamma_{\phi_2}^2)\int_{-\tau}^{0}\|L_ry_h(t+\eta-\tau)\|^2\|e_y(t)\|^2\mathrm{d}\eta \\ & + 2\tau\dot{\beta}_2^2 + 2\tau\dot{\phi}_1^2 + 2\tau^2\dot{\phi}_2^2 + \gamma_2^{-1}\dot{\tilde{\beta}}_2^2\dot{\beta}_3 + 2\gamma_2^{-1}\tilde{\beta}_2\beta_3\dot{\beta}_2 \\ & + 2\gamma_3^{-1}\tilde{\beta}_3\dot{\beta}_3 + 2\gamma_{\phi_1}^{-1}\dot{\phi}_1\tilde{\phi}_1 + 2\gamma_{\phi_2}^{-1}\tau\dot{\phi}_2\tilde{\phi}_2, \end{aligned} \tag{52}$$

where $\tilde{\beta}_2 \triangleq \|\hat{\lambda}_{2max}\| + \beta_2$, $\tilde{\beta}_3 \triangleq \|\hat{\lambda}_{3max}\| + \beta_3$, $\tilde{\phi}_1 \triangleq \|\hat{\Phi}_{1max}\| + \phi_1$, and $\tilde{\phi}_2 \triangleq \|\hat{\Phi}_{2max}\| + \phi_2$. Defining $q \triangleq \lambda_{min}(Q_2)/p$, and rearranging, one can rewrite (52) as

$$\begin{aligned}\dot{V}_2 \le p\|e_y(t)\|^2\Bigg(& -q + \tau\Bigg\{(\mu + 2\gamma_2^2)\|\mathrm{diag}(L_r\mathcal{G}(t-\tau))\|^2 \\ & + (1+2\gamma_{\phi_1}^2)\|x_p(t-\tau)\|^2 + (1+2\gamma_{\phi_2}^2) \\ & \int_{-\tau}^{0}\|L_ry_h(t+\eta-\tau)\|^2\mathrm{d}\eta\Bigg\}\Bigg)\end{aligned}$$

$$+ 2\tau(\dot{\beta}_2^2 + \dot{\phi}_1^2 + \tau\dot{\phi}_2^2) + \gamma_2^{-1}\tilde{\beta}_2^2\dot{\beta}_3 + 2\gamma_2^{-1}\tilde{\beta}_2\beta_3\dot{\beta}_2$$
$$+ 2\gamma_3^{-1}\tilde{\beta}_3\dot{\beta}_3 + 2\gamma_{\phi_1}^{-1}\dot{\phi}_1\tilde{\phi}_1 + 2\gamma_{\phi_2}^{-1}\tau\dot{\phi}_2\tilde{\phi}_2. \quad (53)$$

It follows from Lemma 1 that $x_p(t)$ is bounded, which implies that there exists $\alpha_1 \in \mathbb{R}_+$ such that $\|x_p(t)\|^2 \le \alpha_1$ for all $t \ge t_0$. Since $\|y_h(t)\| \le \|y_o\|$ for all $t \ge t_0$ due to human input saturation, then there exists $\alpha_2 \in \mathbb{R}_+$ such that $\|L_r y_h(t)\|^2 \le \alpha_2$ for all $t \ge t_0$. In addition, as $r(t)$ is bounded, then all the terms in (21) are bounded due to the usage of the projection operator in (27), which implies the boundedness of $\mathcal{G}(t)$ and hence the existence of $\alpha_3 \in \mathbb{R}_+$ such that $\|\text{diag}(L_r\mathcal{G}(t))\|^2 \le \alpha_3$ for all $t \ge t_0$. Therefore, using (53), one can write

$$\dot{V}_2 \le p\|e_y(t)\|^2\Big(-q + \tau\Big\{(\mu + 2\gamma_2^2)\alpha_3 + (1 + 2\gamma_{\phi_1}^2)\alpha_1$$
$$+ (1 + 2\gamma_{\phi_2}^2)\tau\alpha_2\Big\}\Big)$$
$$+ 2\tau(\dot{\beta}_2^2 + \dot{\phi}_1^2 + \tau\dot{\phi}_2^2) + \gamma_2^{-1}\tilde{\beta}_2^2\dot{\beta}_3$$
$$+ 2\gamma_2^{-1}\tilde{\beta}_2\beta_3\dot{\beta}_2 + 2\gamma_3^{-1}\tilde{\beta}_3\dot{\beta}_3 + 2\gamma_{\phi_1}^{-1}\dot{\phi}_1\tilde{\phi}_1$$
$$+ 2\gamma_{\phi_2}^{-1}\tau\dot{\phi}_2\tilde{\phi}_2. \quad (54)$$

Then, there exists a small enough $\tau^* \in \mathbb{R}_+$ such that

$$\tau^*\Big\{(\mu + 2\gamma_2^2)\alpha_3 + (1 + 2\gamma_{\phi_1}^2)\alpha_1 + (1 + 2\gamma_{\phi_2}^2)\tau^*\alpha_2\Big\} < q, \quad (55)$$

which implies, from (54), that for any $\tau \in [0, \tau^*]$, $\dot{V}_2 < 0$ whenever

$$\|e_y(t)\|^2 > \frac{z_1}{z_2}, \quad (56)$$

where

$$z_1 \triangleq 2\tau(\dot{\beta}_2^2 + \dot{\phi}_1^2 + \tau\dot{\phi}_2^2) + \gamma_2^{-1}\tilde{\beta}_2^2\dot{\beta}_3 + 2\gamma_2^{-1}\tilde{\beta}_2\beta_3\dot{\beta}_2$$
$$+ 2\gamma_3^{-1}\tilde{\beta}_3\dot{\beta}_3 + 2\gamma_{\phi_1}^{-1}\dot{\phi}_1\tilde{\phi}_1 + 2\gamma_{\phi_2}^{-1}\tau\dot{\phi}_2\tilde{\phi}_2, \quad (57)$$
$$z_2 \triangleq p\Big(q - \tau\Big\{(\mu + 2\gamma_2^2)\alpha_3 + (1 + 2\gamma_{\phi_1}^2)\alpha_1 + (1 + 2\gamma_{\phi_2}^2)\tau\alpha_2\Big\}\Big). \quad (58)$$

Hence, for any $\tau \in [0, \tau^*]$, the solution $(e_y(t), \tilde{\lambda}_2(t), \tilde{\lambda}_3(t), \tilde{\Phi}_1(t), \tilde{\Phi}_2(t, \eta))$ is bounded and converges to the compact set

$$E \triangleq \Big\{(e_y(t), \tilde{\lambda}_2(t), \tilde{\lambda}_3(t), \tilde{\Phi}_1(t), \tilde{\Phi}_2(t, \eta)) : \|e_y(t)\|^2$$
$$\le \frac{z_1}{z_2}, \|\tilde{\lambda}_2(t)\| \le \tilde{\beta}_2, \|\tilde{\lambda}_3(t)\| \le \tilde{\beta}_3,$$
$$\|\tilde{\Phi}_1(t)\| \le \tilde{\phi}_1, \|\tilde{\Phi}_2(t, \eta)\| \le \tilde{\phi}_2\Big\}. \quad (59)$$

According to (14), since $r(t)$ is bounded, then so is $x_m(t)$. This with the fact that $x_p(t)$ is bounded (by Lemma 1) imply the boundedness of $e_2(t)$. And since $e_y(t) = e_2(t) - e_\Delta(t)$ is bounded, then $e_\Delta(t)$ is also bounded, which implies by (25) that $\Delta y(t)$ is bounded and completes the proof. □

Remark 5. While the existence of the upper bound on the time delay τ^* is guaranteed, its value depends on the selection of the outer-loop learning rates $\gamma_{out} \triangleq \{\gamma_2, \gamma_{\phi_1}, \gamma_{\phi_2}\}$. Note from (55) that as larger values of γ_{out} are used, the allowable maximum time delay τ^* becomes smaller. On the other hand, in the limit where $\gamma_{out} \to 0$, which corresponds to no adaptation, τ^* approaches its ultimate value τ_{max} satisfying

$$\tau_{max}\big(\mu\alpha_3 + \alpha_1 + \tau_{max}\alpha_2\big) < q. \quad (60)$$

On the contrary, the ultimate bound $z \triangleq z_1/z_2$ on the error $e_y(t)$, which is defined by the set (59), (57) and (58), is inversely proportional to the values of γ_{out}. That is, to achieve a better tracking performance, which corresponds to smaller values of z, the outer-loop learning rates γ_{out} should be selected as large as possible. And in the limit where $\gamma_{out} \to \infty$, the upper bound $z \to 0$. Therefore, given any delay value $\tau < \tau_{max}$, the optimal outer-loop learning rates $\gamma_{out,opt}$ are the ones that satisfy $\tau^* = \tau$. A further increase in $\gamma_{out} > \gamma_{out,opt}$ renders our stability analysis inapplicable due to $\tau > \tau^*$, while a decrease in $\gamma_{out} < \gamma_{out,opt}$ allows for higher delay values to be tolerated at the expense of a deteriorated tracking performance.

5 | Simulations

Consider the longitudinal motion of the 747 airplane cruising in level flight at an altitude of 40 kft and a velocity of 774 ft/sec, the perturbation equations of which are represented in the form of (2). The state vector is

$$x_p(t) = \begin{bmatrix} x_{p1}(t) & x_{p2}(t) & x_{p3}(t) & x_{p4}(t) \end{bmatrix}^T, \quad (61)$$

where $x_{p1}(t)$ and $x_{p2}(t)$ are the components of the aircraft's velocity (in ft/s) along the x and z-axes, respectively, with respect to the reference axis, $x_{p3}(t)$ is the aircraft's pitch rate (in crad/s), and $x_{p4}(t)$ is the pitch angle of the aircraft (in crad). The control input $u_p(t)$ represents the elevator deflection (in crad). Under these conditions, nominal dynamics are available in the form of (3), where the nominal system and control input matrices are given as [22]

$$A_n = \begin{bmatrix} -0.0030 & 0.0390 & 0 & -0.3220 \\ -0.0650 & -0.3190 & 7.7400 & 0 \\ 0.0200 & -0.1010 & -0.4290 & 0 \\ 0 & 0 & 1 & 0 \end{bmatrix},$$
$$B_p = \begin{bmatrix} 0.0100 \\ -0.1800 \\ -1.1600 \\ 0 \end{bmatrix}, \quad (62)$$

with the eigenvalues at $-0.3750 \pm 0.8818i$ and $-0.0005 \pm 0.0674i$. The control objective is for a pilot to be able to track a desired trajectory. Particularly, the pilot controls the aircraft to achieve a desired pitch angle $y_2(t) = x_{p4}(t)$. This is done by feeding pitch rate commands through a joystick to the inner-loop, which consists of a control augmentation system designed to track the pilot's pitch rate commands, that is, $y_1(t) = x_{p3}(t)$.

5.1 | Inner Loop: Adaptive Control Augmentation System

The design of the inner-loop adaptive controller starts with the determination of the nominal control law (4), which is used to

define the reference model. Achieving pilot command following by assigning the feed-forward gain L_r as in (6) is not possible since the transfer function $x_{p3}(s)/u_p(s)$ has a zero at the origin. Instead, we design the inner-loop nominal controller by assuming short-period approximation of the nominal dynamics, given by

$$A_{sp} = \begin{bmatrix} -0.3190 & 7.7400 \\ -0.1010 & -0.4290 \end{bmatrix}, \quad B_{sp} = \begin{bmatrix} -0.1800 \\ -1.1600 \end{bmatrix}, \tag{63}$$

where the eigenvalues are at $-0.3740 \pm 0.8824i$, which makes a good approximation of the fast dynamics of (62). Using (63), a feedback gain L_{sp} is designed to place the short-period eigenvalues at -1.5 and -0.5. Then, the feed-forward gain is selected as $L_r = -\left(C_{sp}^T (A_{sp} - B_{sp}L_{sp})^{-1} B_{sp}\right)^{-1}$, where $C_{sp} = [0,\ 1]^T$. The implementation of these values to the full longitudinal dynamics is applied as in (4), where $L_x = [0,\ L_{sp},\ 0]$, allowing for the reference model (5) to be defined using $A_r = A_n - B_p L_x$ and $B_r = B_p L_r$.

An adaptive controller is employed as in (7) and (10) to achieve reference model following in the presence of uncertainty, where the adaptive parameters are initialized at the nominal values $\hat{K}_x(0) = L_x$ and $\hat{\lambda}(0) = 1$. Furthermore, the Lyapunov matrix is selected as $Q_1 = 0.01 I_{4\times4}$, and the learning rates are set to $\gamma_x = \text{diag}([0.01,\ 0.001,\ 0.01,\ 0.01])$ and $\gamma_\lambda = 0.001$.

5.2 | Outer Loop: Adaptive Pilot Model

For the outer loop, the proposed adaptive human pilot model is employed as in (14), (19), (20), (21), (25), and (27), where manipulator limits of ± 10 crad/s (i.e., $y_o = 10$) are imposed on the pilot's input. Reflecting the overall nominal response, the crossover-reference model (14) defines how a well-trained pilot controls the aircraft under nominal circumstances, providing satisfactory performance and adequate stability margins. While its determination is application-dependent and can require experimental analysis, to serve the purpose of this section, we define the crossover-reference model using the LQR method by calculating θ_x using $Q_{LQR} = \text{diag}([0,\ 0.01,\ 0.6,\ 10])$ and $R_{LQR} = 0.6$, with θ_r given in (15), and assigning $A_m = A_r - B_r\theta_x$, and $B_m = B_r\theta_r$.

The time delay τ in the pilot's response to visual stimuli can be broken down into approximate components [14] constituting the latency of the visual process (≈ 0.075 s), the motor nerve conduction time (≈ 0.030 s), and the central processing time (≈ 0.030 s). While exact values may vary depending on the pilot's attention, these average values are convenient for use in this section, yielding a total delay of $\tau = 0.135$ s in the pilot's response.

The finite integral term in (21) and the adaptive law (27d) are implemented by discretizing the integral into 5 intervals as illustrated in [23]. The outer-loop adaptive parameters are initialized at the nominal values $\hat{\lambda}_2(0) = \hat{\lambda}_3(0) = 1$, $\hat{\Phi}_1(0) = -\theta_x e^{A_r\tau}$, and $\hat{\Phi}_2(0,\eta) = -\theta_x e^{-A_r\eta} B_p$. This initialization implies that the pilot initially starts with the nominal control law

$$v_n(t) = -\theta_x x_n(t+\tau) + \theta_r r(t), \tag{64a}$$

$$x_n(t+\tau) = e^{A_r\tau} x_p(t) + \int_{-\tau}^{0} e^{-A_r\eta} B_r y_h(t+\eta)\, \mathrm{d}\eta, \tag{64b}$$

$$y_{hn}(t) = \begin{cases} v_n(t), & \text{if } |v_n(t)| \le y_o, \\ y_o \text{sgn}(v_n(t)), & \text{if } |v_n(t)| > y_o, \end{cases} \tag{64c}$$

which matches the crossover-reference model in the absence of plant uncertainty and input saturation. Finally, the Lyapunov matrix is selected as $Q_2 = 0.01 I_{4\times4}$, and the outer-loop learning rates are set to $\gamma_2 = 0.5$, $\gamma_3 = 1000$, $\gamma_{\phi_1} = \text{diag}([0.01,\ 0.01,\ 0.1,\ 0.1])$, and $\gamma_{\phi_2} = 0.01$.

5.3 | Failure Scenario

In the simulated scenario, we start with $\Lambda = 1$ and an uncertainty in the modeled dynamics with the system matrix

$$t < 30:\ A_p = \begin{bmatrix} -0.0067 & 0.0410 & -0.0037 & -0.3223 \\ 0.0010 & -0.3558 & 7.8068 & 0.0047 \\ 0.4454 & -0.3380 & 0.0015 & 0.0302 \\ 0 & 0 & 1 & 0 \end{bmatrix}, \tag{65}$$

placing the eigenvalues at $-0.1800 \pm 1.6000i$ and $-0.0005 \pm 0.1400i$. An anomaly is then introduced into the inner-loop controller at $t = 20$ s, failing the adaptation in the $\hat{K}_x(t)$ channel (i.e., $\gamma_x = 0_{4\times4}$ for $t \ge 20$ s). It is noted that the other inner-loop adaptive parameter, $\hat{\lambda}(t)$, is kept actively adapting throughout the simulation. At $t = 30$ s, a failure is introduced into the plant dynamics, where the control effectiveness reduces to $\Lambda = 0.5$ for $t \ge 30$ s, and the system matrix becomes

$$t \ge 30:\ A_p = \begin{bmatrix} -0.0127 & 0.0427 & -0.0040 & -0.3227 \\ 0.1100 & -0.3859 & 7.8124 & 0.0131 \\ 1.1479 & -0.5323 & 0.0376 & 0.0847 \\ 0 & 0 & 1 & 0 \end{bmatrix}, \tag{66}$$

placing the eigenvalues at $-0.1800 \pm 2.0000i$ and $-0.0005 \pm 0.1750i$.

Figure 2 shows the pitch angle tracking trajectory for the aforementioned scenario, where the performance of the proposed adaptive pilot model is compared with a fixed (non-adaptive) pilot model utilizing the nominal control law (64). The effectiveness of adaptation in the proposed model is evident as it learns to compensate for the plant failure, converging back to the desired trajectory of the crossover-reference model. On the other hand, for the nominal pilot model, the plant failure causes a permanent deviation from the desired trajectory, which persists since the model is non-adaptive and is therefore a poor representation of what a well-trained pilot would do in such a situation.

The pitch angle tracking error and pilot inputs are displayed in Figure 3 for both the nominal and the adaptive models, and the evolution of the human adaptive parameters is displayed in Figure 4. While the adaptive model achieves enhanced transients, it comes at the expense of an increase in the pilot control effort. This can be observed from Figure 3, particularly in the time frame

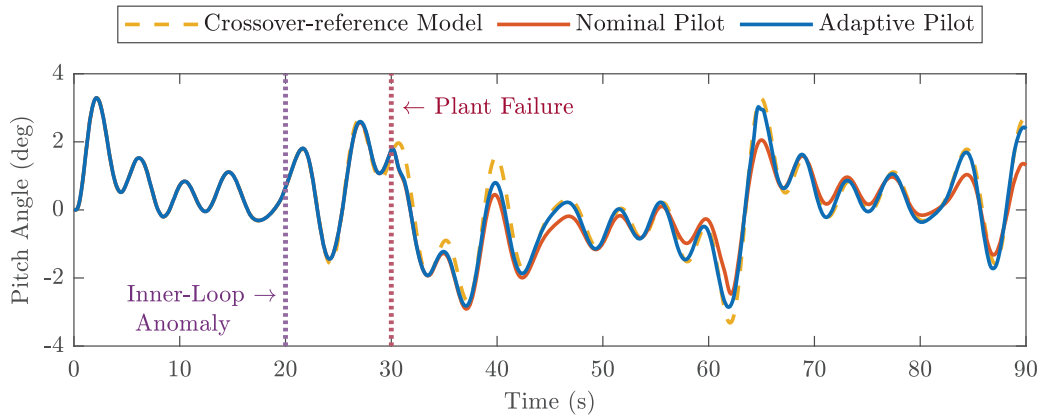

FIGURE 2 | Pitch angle trajectory tracking of the proposed adaptive model, compared with a nominal non-adaptive pilot model.

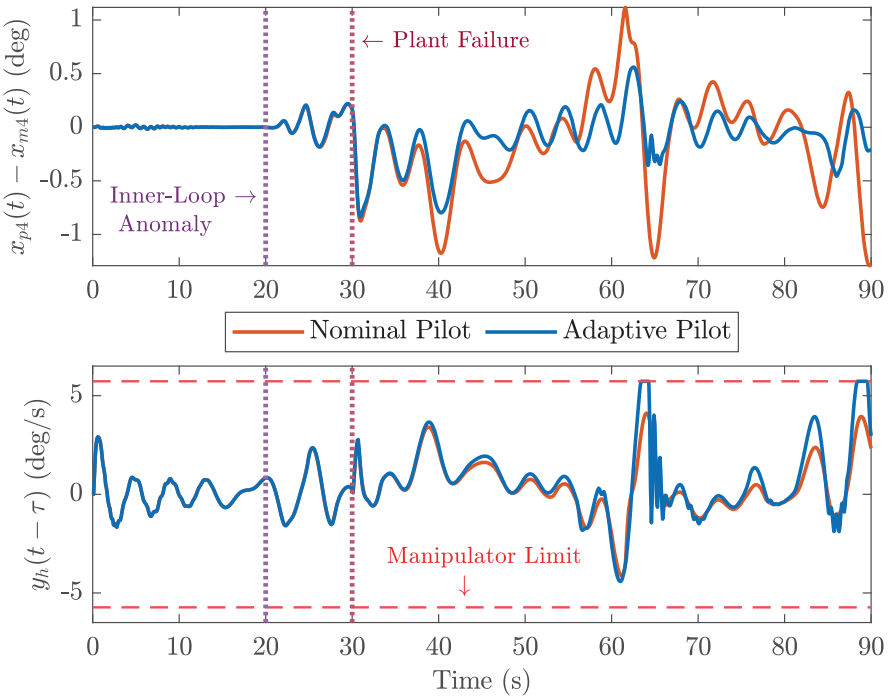

FIGURE 3 | Top: Pitch angle tracking error evolution. Bottom: Pilot control inputs.

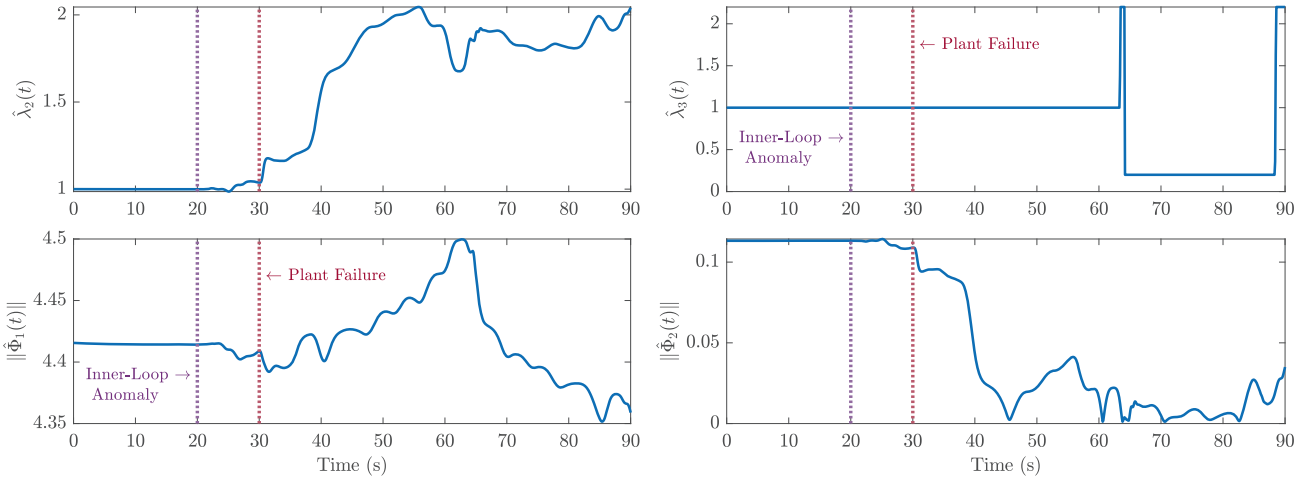

FIGURE 4 | Evolution of the human adaptive parameters. The norm $\|\hat{\Phi}_2(t)\|$ is computed across the 5 discrete points in η, that is, $\|\hat{\Phi}_2(t)\| = (\sum_{i=1}^{5} \hat{\Phi}_2(t, \eta_i)^2)^{1/2}$.

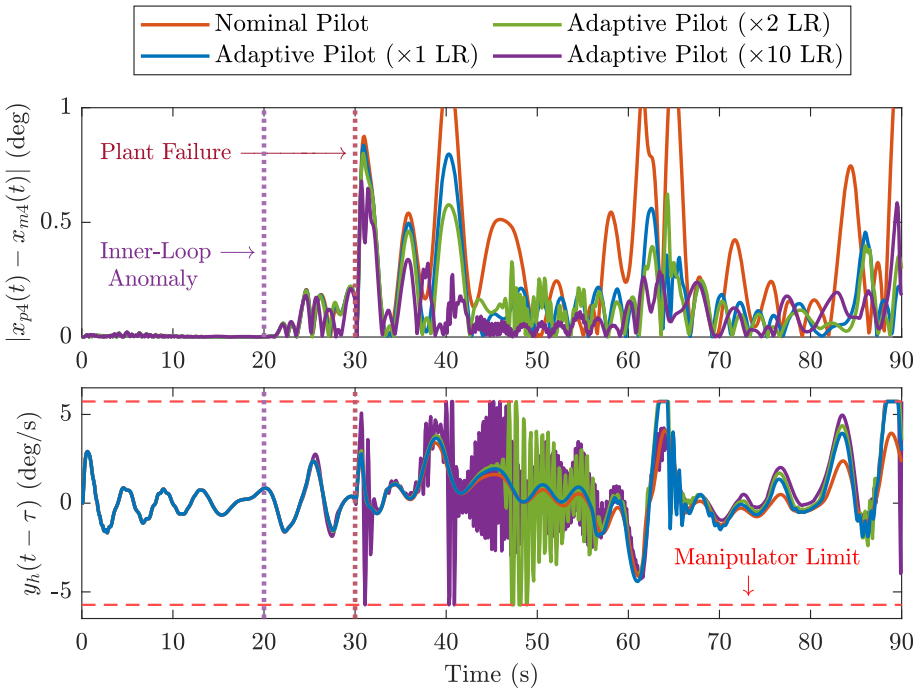

FIGURE 5 | Pitch angle tracking error (top) and pilot control inputs (bottom) for the nominal pilot model and the adaptive pilot model with different learning rate values. The adaptive pilot model (×1 LR), whose signals are also shown in Figures 2–4, uses the learning rates $\gamma_2, \gamma_3, \gamma_{\phi_1}, \gamma_{\phi_2}$ specified at the end of Section 5.2, while the adaptive pilot models (×2 LR) and (×10 LR) use double and ten times each of these rates, respectively.

between 63 – 67 seconds, where the control inputs of the adaptive model are more oscillatory than those of the nominal one, but leading to a 70% reduction in the pitch angle tracking error. Under the effect of a failure, such a behavior can be expected from a pilot attempting to compensate for the uncertainty, which also raises the question of how to better design the control system by taking the human pilot into consideration.

Finally, to investigate how tuning the human learning rates affects human adaptation, Figure 5 shows the pitch angle tracking error and pilot control inputs for the nominal pilot model and the adaptive pilot model with different learning rate values. As expected, higher human learning rates lead to faster human adaptation, resulting in lower pitch tracking error. However, this comes at the cost of increased human control effort. Therefore, when modeling human behavior, it is crucial to select learning rates that reflect realistic adaptation speeds while maintaining control efforts representative of those observed in real pilots.

6 | Conclusions

This paper introduces an adaptive human pilot model designed to capture a pilot's behavior in the loop with an adaptive controller. The pilot is modeled using a model reference adaptive control architecture accounting for reaction time delay and input saturation, and supported by a rigorous Lyapunov–Krasovskii stability analysis. The effectiveness of the proposed adaptive pilot model is validated through a detailed simulation study of the longitudinal motion of a 747 airplane, demonstrating that the proposed adaptive pilot model provides a more accurate representation of a well-trained pilot compared to a fixed nominal pilot model. The adaptive pilot model serves as a valuable tool for guiding the design of adaptive controllers and enabling their evaluation in simulation environments to ensure safe pilot-controller interactions.

Funding

This work was supported by the Turkish Academy of Sciences under the Young Scientist Award Program.

Conflicts of Interest

The authors declare no conflicts of interest.

Data Availability Statement

Data sharing is not applicable to this article as no datasets were generated or analysed during the current study.

References

1. K. S. Narendra and A. M. Annaswamy, *Stable Adaptive Systems* (Courier Corporation, 2012).

2. E. Lavretsky and K. Wise, *Robust and Adaptive Control: With Aerospace Applications* (Springer, 2013).

3. D. Klyde, C. Y. Liang, D. Alvarez, N. Richards, R. Adams, and B. Cogan, "Mitigating Unfavorable Pilot Interactions With Adaptive Controllers in the Presence of Failures/Damage," in *AIAA Atmospheric Flight Mechanics Conference* (AIAA, 2011), 6538.

4. D. McRuer and D. Graham, "Pilot-Vehicle Control System Analysis," in *Guidance and Control Conference* (AIAA, 1963), 310.

5. M. Lone and A. Cooke, "Review of Pilot Models Used in Aircraft Flight Dynamics," *Aerospace Science and Technology* 34 (2014): 55–74.

6. S. Xu, W. Tan, A. V. Efremov, L. Sun, and X. Qu, "Review of Control Models for Human Pilot Behavior," *Annual Reviews in Control* 44 (2017): 274–291.

7. R. A. Hess, "Modeling Pilot Control Behavior With Sudden Changes in Vehicle Dynamics," *Journal of Aircraft* 46, no. 5 (2009): 1584–1592.

8. R. A. Hess, "Modeling Human Pilot Adaptation to Flight Control Anomalies and Changing Task Demands," *Journal of Guidance, Control, and Dynamics* 39, no. 3 (2016): 655–666.

9. S. S. Tohidi and Y. Yildiz, "A Control Theoretical Adaptive Human Pilot Model: Theory and Experimental Validation," *IEEE Transactions on Control Systems Technology* 30, no. 6 (2022): 2585–2597.

10. T. Yucelen, Y. Yildiz, R. Sipahi, E. Yousefi, and N. Nguyen, "Stability Limit of Human-In-The-Loop Model Reference Adaptive Control Architectures," *International Journal of Control* 91, no. 10 (2018): 2314–2331.

11. E. Arabi, T. Yucelen, R. Sipahi, and Y. Yildiz, "Human-In-The-Loop Systems With Inner and Outer Feedback Control Loops: Adaptation, Stability Conditions, and Performance Constraints," in *AIAA Scitech 2019 Forum* (AIAA, 2019), 2183.

12. S. Tohidi and Y. Yildiz, "Adaptive Control Allocation: A Human-In-The-Loop Stability Analysis," *IFAC-PapersOnLine* 53, no. 2 (2020): 6321–6326.

13. A. Habboush and Y. Yildiz, "An Adaptive Human Pilot Model for Adaptively Controlled Systems," *IEEE Control Systems Letters* 6 (2021): 1964–1969.

14. R. A. Hess, "Structural Model of the Adaptive Human Pilot," *Journal of Guidance and Control* 3, no. 5 (1980): 416–423.

15. A. Habboush and Y. Yildiz, "An Adaptive Pilot Model With Reaction Time-Delay," in *2022 IEEE 61st Conference on Decision and Control (CDC)* (IEEE, 2022), 38–43.

16. M. Y. Uzun, E. Inanc, and Y. Yildiz, "A Robust Human-Autonomy Collaboration Framework With Experimental Validation," *IEEE Control Systems Letters* 8 (2024): 2313–2318.

17. S. S. Tohidi, Y. Yildiz, and I. Kolmanovsky, "Adaptive Control Allocation for Constrained Systems," *Automatica* 121 (2020): 109161.

18. S. P. Karason and A. M. Annaswamy, "Adaptive Control in the Presence of Input Constraints," in *1993 American Control Conference* (IEEE, 1993), 1370–1374.

19. M. Schwager and A. M. Annaswamy, "Direct Adaptive Control of Multi-Input Plants With Magnitude Saturation Constraints," in *Proceedings of the 44th IEEE Conference on Decision and Control* (IEEE, 2005), 783–788.

20. W. J. Rugh, *Linear System Theory*, 2nd ed. (Prentice-Hall, Inc., 1996).

21. C. T. Chen, *Linear System Theory and Design*, 3rd ed. (Oxford University Press, Inc, 1998).

22. A. E. Bryson, *Control of Spacecraft and Aircraft* (Princeton university press, 1994).

23. Y. Yildiz, A. M. Annaswamy, D. Yanakiev, and I. Kolmanovsky, "Spark-Ignition-Engine Idle Speed Control: An Adaptive Control Approach," *IEEE Transactions on Control Systems Technology* 19, no. 5 (2010): 990–1002.